NONLINEAR OPTICAL PHENOMENA

Broadband picosecond radiation source based on noncollinear optical parametric amplifier

V.G. Arakcheev, A.K. Vereshchagin, K.A. Vereshchagin, V.B. Morozov, V.G. Tunkin, D.V. Yakovlev

Abstract. **Amplification of broadband radiation of modeless dye laser by a noncollinear optical parametric amplifier based on a KTP crystal has been implemented upon pumping by 63-ps second-harmonic pulses of a Nd : YAG laser. Pulses with a bandwidth of 21 nm, a duration of 26 ps and an energy of 1.2 mJ have been obtained at the centre wavelength of 685 nm.**

Keywords: picosecond pulses, noncollinear parametric amplifier, broadband lasing.

1. Introduction

Broadband radiation (covering several tens or even hundreds of nanometres) is used in some spectroscopic methods. Simultaneous detection of signals in different spectral regions makes it possible to significantly reduce the time necessary for recording data and to simultaneously increase the accuracy and reproducibility of measurements. Broadband optical radiation sources are applied in different versions of absorption spectroscopy. Currently, nonlaser sources, such as LEDs [1, 2] (which emit in different spectral regions and have emission bands of several tens of nanometres) and deuterium and xenon lamps [3–5], are still efficiently used to estimate the content of harmful impurities in atmosphere.

A universal way for obtaining broadband pulses with durations in the ranges from subnanosecond to femtosecond is the generation of a supercontinuum. To implement it, one can focus laser pulses into a layer of a transparent condensed material (heavy water, ethylene glycol, carbon tetrachloride, fused or crystalline quartz, etc.) [6]. Recently photonic crystal fibres have been widely used to generate a supercontinuum [7]. A supercontinuum with a band ranging from 600 to 1600 nm, generated in a photonic-crystal fibre as a result of introduction of subnanosecond 1064-nm pulses into it, was

V.G. Arakcheev, V.B. Morozov Department of Physics,
M.V. Lomonosov Moscow State University, International Laser Center, M.V. Lomonosov Moscow State University, Vorob'evy gory, 119991 Moscow, Russia; e-mail: morozov@phys.msu.ru;
A.K. Vereshchagin, K.A. Vereshchagin A.M. Prokhorov General Physics Institute, Russian Academy of Sciences, ul. Vavilova 38, 119991 Moscow, Russia;
V.G. Tunkin, D.V. Yakovlev Department of Physics, M.V. Lomonosov Moscow State University, Vorob'evy gory, 119991 Moscow, Russia; e-mail: vgtunkin@mail.ru, dmyak@physics.ru

applied in [8] to record absorption spectra of water vapour in atmosphere. Quantitative detection of trace gas impurities was performed by highly sensitive absorption spectroscopy in a frequency band from 620 to 740 nm, selected from the extended spectrum of the supercontinuum generated in a photonic-crystal fibre [9]. With the use of 5-ps pulses of a master ytterbium-doped fibre laser, the supercontinuum pulse duration in an isolated band was estimated to be 200 ps. In addition, the supercontinuum from chirped, extended in time, and amplified pulses of an ytterbium-doped fibre laser (700–1700 nm, 300 ps), obtained in a photonic-crystal fibre, was applied to record absorption spectra and study the laser-stimulated breakdown in microplasma channels [10].

Near-field microscopy allows one to study the surface structure of organic materials by analysing images recorded with the aid of broadband radiation in different spectral ranges, with a spatial resolution exceeding the diffraction limit [11].

Broadband radiation sources are actively used to study molecules on the surface of materials or near the interface between different media; this analysis is performed by sum-frequency spectroscopy [12–16]. Examples of vibrational spectra of molecules adsorbed on a surface, recorded in the spectral range from 200 cm^{-1} (CO/Rb, CO/Pt, CN$^-$/Ag) to 1000 cm^{-1} (water vapour/water or solutions) and even to 2000 cm^{-1} (C$_{60}$/Ag), were presented in review [12]. The formation of spectral distributions during one laser pulse in a frequency band of 250 cm^{-1} in the study of the self-assembly of molecular layers on a gold surface excludes the necessity of scanning and allows one to avoid signal distortions, which are caused by amplitude fluctuations and spatial beam overlap [13, 14]. Under these conditions, broadband lasing with a centre wavelength of 3400 nm and a single-pulse energy of few microjoules occurs as a result of optical parametric amplification and subsequent generation of a difference-frequency signal from the signal and idler waves.

One of the widespread methods based on the use of broadband recording spectra is the coherent anti-Stokes Raman scattering (CARS) [17]. One of its modifications is the dual broadband pure rotational CARS [18]. In this scheme, coherent excitation of low-frequency pure rotational Raman-active transitions is performed by a pair of identical pulses with a wide spectrum, covering many lines of the rotational structure (several hundreds of inverse centimetres, a value determined by the typical width of rotational bands), which converge in the interaction volume at a small angle, whereas the probe pulse has a rather narrow spectrum. It is convenient to use modeless dye lasers with necessary amplification cascades as broadband radiation sources in CARS spectroscopy and

its modifications [19, 20]. Modeless laser radiation possesses no mode structure [21], which is important for uniform excitation and correct determination of the ratio of rotational component amplitudes in the CARS spectra of molecular gases [22].

Recently a modification of broadband CARS based on the use of picosecond [23–25] or femtosecond [26] excitation pulses has become popular. The introduction of a short delay between the excitation and probe pulses makes it possible to exclude the nonresonant background (caused by the electron-subsystem contribution [17]) from the recorded signal [27]. At the same time, the relatively small spectral width of the picosecond probe pulse allows one to separate the resonant contributions from different spectral components to the recorded signal.

The spectral bandwidth of excitation pulses, which is necessary to record, for example, the rotational spectrum of molecular nitrogen at temperatures up to 2500 K, should be not smaller than 400 cm^{-1} [23] (a value multiply exceeding the bandwidth of the probe pulse, which can also be spectrally limited). Note that a significant excess above the optimal excitation bandwidth is also undesirable because of possible excitation of the related nonlinear processes contributing to the signal in the same spectral region [27]. In this context, the use of femtosecond pulses may be less convenient in some cases. An optimal solution in this case is the application of picosecond pulses with a fairly large bandwidth. Concerning the pulse energy that is necessary, for example, for broadband picosecond CARS spectroscopy of molecular gases, the optimal values amount to several millijoules [28] due to the nonlinear character of interaction [17]; i.e., are much smaller than those required for nanosecond CARS spectroscopy [18–20].

Thus, the design of efficient broadband picosecond radiation sources emitting in a specified spectral range is an urgent problem. Selection of the optimal spectral and temporal characteristics of radiation, depending on the class of objects under study and the spectroscopic scheme used, is performed individually in each case.

To obtain amplified radiation in a certain (fairly wide) frequency band, for example, in order to solve some problems in amplification of femtosecond pulses, many researchers used noncollinear optical parametric amplifiers (NOPAs). Isaenko et al. [15] amplified supercontinuum radiation (generated in a sapphire plate by 55-fs pulses at a wavelength of 800 nm) using an NOPA based on a KTP crystal, pumped by pulses of the same duration and at the same wavelength. Radiation tunable in the range of 1100–1500 nm with a ∼1000-cm^{-1} band (λ = 1200 nm) was obtained in the form of a train of pulses similar to transform-limited ones, with a duration of 25 fs, an energy up to 44 nJ and a repetition rate of 250 kHz. Master oscillator pulses with the same wavelength (800 nm) but a duration of 140 fs and a much higher energy were used to pump a two-cascade NOPA based on LiNbO$_3$ and KNbO$_3$ crystals in [16]. The generated pulses, tunable in the range of 1800–3500 nm and having a bandwidth of ∼600 cm^{-1} (λ = 3500 nm), along with the narrow-band pulses at the oscillator wavelength, made it possible to implement sum-frequency spectroscopy for studying the vibrational spectra of water molecules absorbed on a quartz surface. To obtain high-power femtosecond radiation near 1.5 μm, chirped pulses of an erbium-doped fibre laser were amplified in an NOPA based on a KTiOAsO$_4$ (KTA) crystal, with pumping by 100-ps Nd:YLF laser pulses [29]. Pulses with a duration of 130 fs and an energy of 500 μJ were obtained at the compres-

sor output. Chirped pulses with an energy of 38 J and a centre wavelength of 910 nm were obtained using a three-cascaded system of broadband parametric amplifiers based on KD*P crystals [30]. Here, a femtosecond fibre laser generating a train of pulses with a wavelength of 1250 nm, a duration of 40 fs and an energy of 2 nJ was used as a master source. The first two cascades were pumped by second-harmonic pulses of a nanosecond Nd:YLF laser with a Nd:YLF amplifier. The third cascade was pumped by pulses from the output of a neodymium glass amplifier, converted into the second harmonic. Pulses with a duration of 43 fs and an energy of 24 J were obtained at the compressor output.

The parametric gain can be fairly large. For example, a gain of 10^8 was reached for a KTA-based NOPA in [29]. The gain of a cw single-frequency semiconductor laser in a two-cascade parametric amplifier based on LiNbO$_3$ crystals, pumped by picosecond pulses of a Nd:YAG laser, was as high as 10^9 [31], and transform-limited pulses with a duration of 18 ps and an energy of 2 mJ were obtained at a wavelength of 1400 nm. A similar approach was used to generate tunable transform-limited picosecond pulses at a wavelength of 566 nm in an optical parametric oscillator based on a BBO crystal [32], into which seed 950-nm radiation from a semiconductor laser was injected.

The above-considered examples [15, 16, 29–31] indicate that the requirements to the duration of pump pulses for a parametric amplifier and to the gain spectral range may significantly differ, depending on a specific problem to be solved. For example, when amplifying time-extended chirped pulses [29, 30], pump pulses are generally chosen much longer than the amplified ones. Here, the desired width of the gain spectral range is basically determined by the bandwidth of the initial femtosecond pulses. In the case of parametric amplification of cw broadband seed radiation [31, 32], the duration of the generated pulses is generally determined by the pump pulse duration. The same holds true for the pulse bandwidth. If both the amplified radiation and NOPA pump radiation have the same origin [15, 16], the resulting pulses may be much shorter than the initial ones. To avoid spectral narrowing during amplification, the phase-matching range should be sufficiently wide; this condition can be satisfied by choosing an appropriate parametric converter.

Thus, application of NOPAs for generating broadband picosecond pulses with a rather high power in the desired spectral range appears to be quite justified. The radiation of a modeless source (supercontinuum generator, dye laser, or superluminescent diode) can be used as a broadband seed to be amplified. The purpose of our study was to obtain picosecond radiation with a bandwidth of about 400 cm^{-1} and an energy of ∼1 mJ by amplifying the radiation of a modeless dye laser in a noncollinear parametric amplifier under picosecond pumping.

2. Experimental

A schematic of the experimental setup is shown in Fig. 1. A picosecond LS-2151 laser (LOTIS TII), composed of a master Nd:YAG oscillator with a pulse duration of 75 ps at a wavelength of 1064 nm and a second-harmonic converter, operated with a repetition rate up to 10 Hz. The second-harmonic radiation with a wavelength of 532 nm and an energy of 11 mJ was split into two parts. The first part, with an energy of 2.3 mJ, was used to pump a dye laser, while the second part, with an energy of 8.7 mJ, pumped a parametric amplifier

based on a KTP crystal. The pump radiation was focused by cylindrical lens L5 with a focal length of 5 cm into a cell filled with a pyridine dye solution in ethanol. A transversely pumped modeless dye laser was implemented using mirror M1, according to the scheme of double-pass amplifier of spontaneous luminescence. The laser generated radiation with a bandwidth of 24 nm (520 cm^{-1}), a centre wavelength 685 nm, and an energy per pulse of about 10 µJ. The choice of the dye type was determined, in particular, by the possibility of realising vibrational–rotational CARS in hydrogen at the aforementioned centre wavelength [19]. The fact that the broadband radiation wavelength falls in the red spectral region is also convenient for dual broadband CARS.
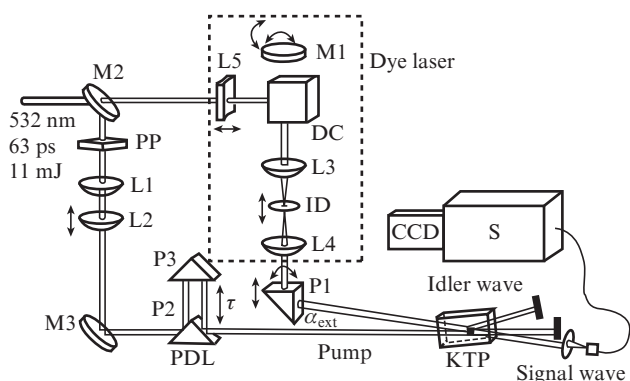

Figure 1. Schematic of the experimental setup: (L1–L4) spherical lenses; (L5) cylindrical lens; (M1–M3) mirrors; (DC) cell filled with a dye solution; (ID) iris diaphragm; (PP) phase plate (which rotates the second-harmonic's plane of polarisation by 90°); (P1–P3) prisms; (PDL) prism delay line; (S) spectrograph with a fibre input; α_{ext} is the external noncollinearity angle.

We used a KTP crystal ($4 \times 6 \times 10$ mm in size), cut so as to implement the scheme of collinear interaction between the pump ($\lambda_p = 532$ nm), signal ($\lambda_s = 670$ nm) and idler ($\lambda_i = 2583$ nm) waves in the ZX (horizontal) plane. Under normal incidence of a pump wave on the input face of the crystal, the angle θ_p between the Z axis of the crystal and the pump wave vector was $46 \pm 1°$. To provide noncollinear interaction between the light waves, the crystal was rotated around the vertical axis by a corresponding angle. We used the ooe-type interaction (where the pump and idler waves are ordinary and the signal wave is extraordinary). The output radiation of the pump laser at a wavelength of 532 nm was horizontally polarised; therefore, to form an o-polarised pump beam, a half-wave plate PP was installed after beam-splitting mirror M2; this plate served to rotate the second-harmonic polarisation vector by 90°. This radiation (with an initial beam diameter of 8 mm) formed a pump beam (2.7 mm in diameter) for the parametric amplifier using a telescope composed of lenses L1 and L2, with focal lengths of 300 and –100 mm, respectively. A delay line based on prisms P2 and P3 was installed in the pump channel of the parametric amplifier to provide temporal matching of the pump and dye laser pulses in the KTP crystal. The pump, signal, and idler waves were spatially separated at the output of the crystal in a natural way due to the noncollinear interaction: the pump and idler waves were blocked, while the signal wave (amplified dye laser radiation) was directed by an optical fibre to a spectrograph or streak camera.

3. Broadband parametric amplification

As was noted in a number of studies devoted to parametric amplification under femtosecond or picosecond pumping [33, 34], enhancement of parametric luminescence is observed in the directions in the amplifier crystal in which the group-phase-matching condition is satisfied. Figure 2 shows the image of amplified dye laser radiation on a screen located at a distance of 40 cm from the NOPA crystal. The image in Fig. 2a was obtained by reducing the dye laser radiation before the input of the KTP crystal by a factor of 200 (using neutral light filters). The image contains a parametric-luminescence ring, corresponding to the signal-wave spectral range. Some azimuthal modulation of parametric luminescence intensity, which was repeated from shot to shot, is apparently related to the spatial distribution of pump radiation.
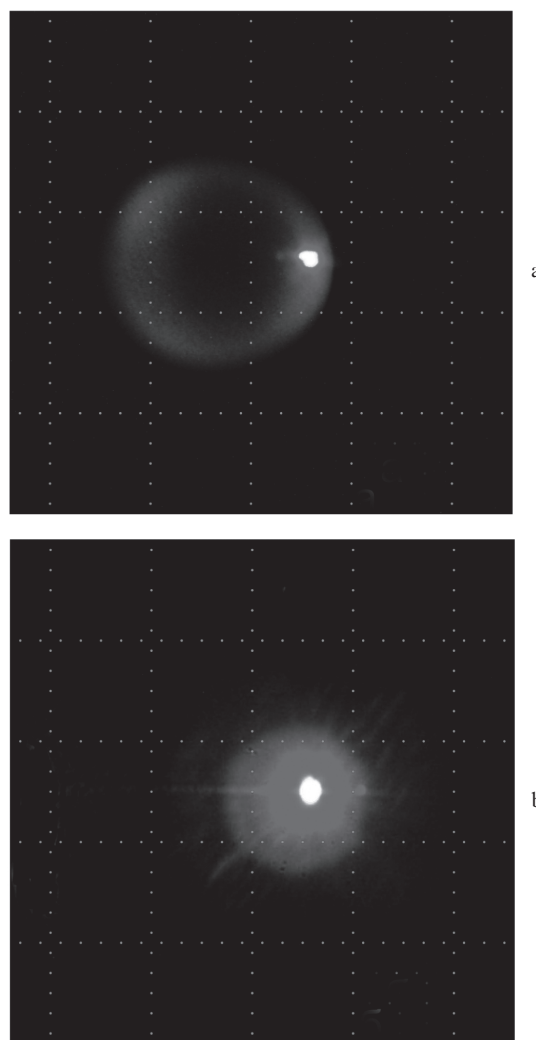

Figure 2. (a) Parametric luminescence and amplified radiation of dye laser after its reduction by a factor of 200 by neutral light filters at the input in KTP crystal and (b) amplified dye radiation in the absence of neutral light filters. The image-field transverse size is 10 cm.

We calculated the dependences of the wavelength λ_s of signal wave on the angle θ_p between the pump beam and Z axis for several internal noncollinearity angles α_{int} (Fig. 3). The
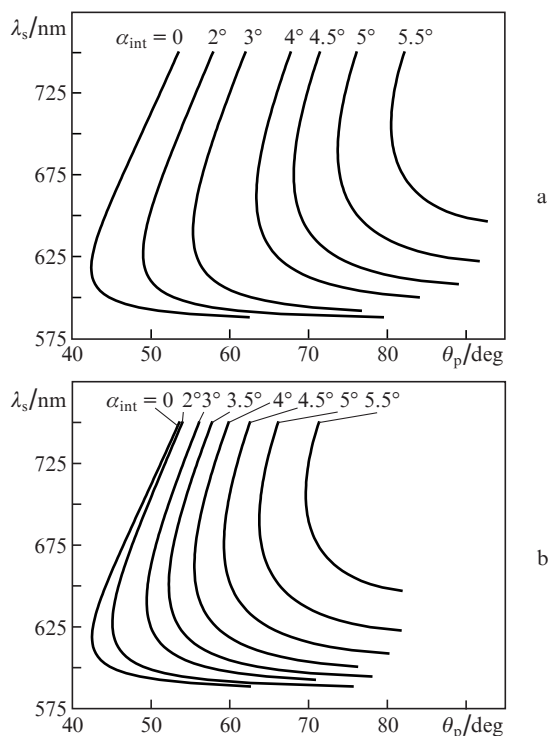
Figure 3. Dependence of the signal-wave length λ_s on the angle θ_p between the Z axis and the pump wave vector with $\lambda p = 532$ nm under phase-matching conditions in the XZ plane of KTP crystal at different noncollinearity angles α_{int} in the cases of location the signal wave vector (a) between the Z axis and the pump wave vector and (b) between the X axis and the pump wave vector.

refractive indices were calculated from the Sellmeier formulas [35]. Two cases were considered: the signal wave propagates (i) within and (ii) beyond the angle between the Z axis and the pump beam. Our experimental conditions correspond to the second case (Fig. 3b).

The parametric phase-matching width in the minimum θ_{min} of the dependence $\theta_p(\lambda_s)$ is determined by the second derivative $(d^2\theta/d\lambda^2)_{\theta_{min}}$: the smaller the second derivative, the smaller the slope of the dependence of the angle θ_p on the wavelength λ_s and, therefore, the wider the parametric phase matching. Figure 4 shows the second derivative $(d^2\theta/d\lambda^2)_{\theta_{min}}$ in the minimum θ_{min} as a function of the internal noncol-
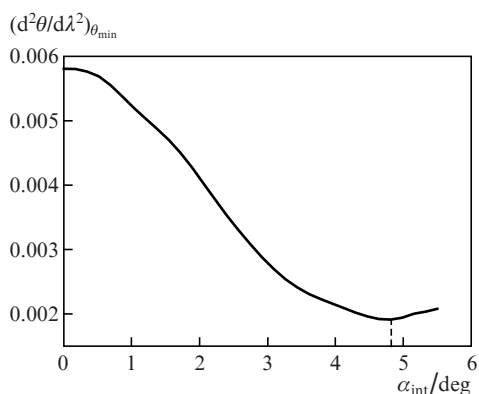
linearity angle α_{int}. As follows from the calculations, the maximum width of parametric phase matching and, therefore, parametric gain spectrum correspond to $\alpha_{int} \sim 4.5-5°$; in this case, the phase-matching angle θ_p should be $59-64°$. Under these conditions, the dye laser spectrum is minimally narrowed during amplification.

The pump-beam incidence angle into the crystal and the angle between the pump and dye laser beams were chosen experimentally in the following way. The parametric luminescence radiation, propagating to the right in the XZ plane, was coupled into the optical fibre and then applied to an MDR-6 spectrograph. The parametric luminescence wavelength was tuned to the dye laser centre wavelength (685 nm) by rotating the KTP crystal in the XZ plane; under these conditions, the angle between the pump beam and the direction in which the parametric luminescence intensity was maximum (see Fig. 2a) changed, and the optical fibre was correspondingly displaced. As a result, the angle between the normal to the surface and the pump beam direction was about $24°$. The angle between the Z axis and the pump beam in the crystal was, therefore, $\sim60°$, a value corresponding to the aforementioned optimal values of the phase-matching angle: $59-64°$.

The angle of incidence of the dye laser beam (aligned with the pump beam in the KTP crystal) on the crystal was chosen so as to make the beam outgoing from the crystal to enter the optical fibre, which was tuned to 685-nm parametric luminescence. The broadband dye laser radiation injected at this angle was efficiently amplified. After removing neutral light filters, the amplified beam (signal wave) spot became much brighter, an intense halo was observed around it, and the parametric luminescence brightness decreased so that could not be recorded by the camera (see Fig. 2b).

The pump pulse energy at the input of the KTP crystal was measured by an IMO-2 power meter to be 8.7 mJ. With allowance for the reflection from the input surface (having no antireflection coating) of the KTP crystal (the refractive index of which is ~1.8), the real energy of the pump pulse was 8 mJ. The signal-wave pulse energy turned out to be 1.2 mJ; thus, we obtained 15% conversion of the pump energy into the signal-wave energy. Note a significant improvement of the spatial quality of the amplified signal beam in comparison with the initial beam. The spectral FWHM was 21 nm (450 cm^{-1}). The measured spectra of the initial and amplified beams are shown in Fig. 5, and the temporal profiles of
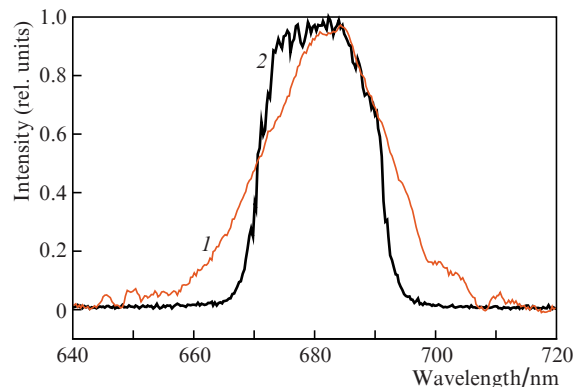
Figure 4. Dependence of $(d^2\theta/d\lambda^2)_{\theta_{min}}$ on the internal noncollinearity angle α_{int}.

Figure 5. (*1*) Initial spectrum of dye laser radiation [bandwidth 24 nm (520 cm^{-1})] and (*2*) the spectrum of radiation at the output of parametric amplifier [21 nm (450 cm^{-1})].
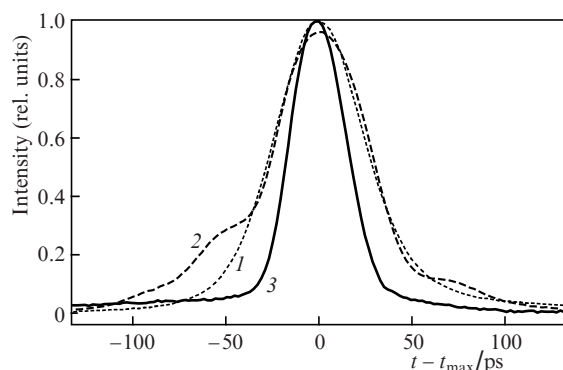
Figure 6. Temporal profiles of pulses: (*1*) the second harmonic of Nd:YAG laser (duration 63 ps), (*2*) dye laser (57 ps), and (*3*) amplified dye laser radiation (26 ps).

signals are presented in Fig. 6. The amplified pulse (with a duration of 26 ps) is much shorter than the initial dye laser and pump pulses (57 and 63 ps, respectively).

In our opinion, the NOPA used as a source of picosecond pulses to solve nonlinear-spectroscopy problems (in particular, in dual broadband CARS spectroscopy) has a number of undoubted advantages. These are high gain, possibility of significant shortening the amplified pulse in comparison with the pump pulse, and the high contrast with respect to the noise caused by spontaneous parametric scattering (the temporal profile of amplified radiation barely contains any background, which is inherent in laser amplifiers and caused by active-medium luminescence). Note that radiation of any other laser or broadband superluminescent source, including cw sources (for example, a superluminescent semiconductor diode), can be used to perform injection into picosecond NOPA. Different types of superluminescent diodes used in optical coherent tomography were reviewed in [36]. The bandwidth of these diodes reaches 60 nm, the power is in the range from several units to several tens of milliwatts, and the centre wavelength ranges from 660 to 1600 nm. Alignment of beams from two superluminescent diodes with somewhat shifted spectra made it possible to expand the emission spectrum up to 100 nm (with conservation of its bell-shaped profile) [37].

When pumping by the second harmonic of a Nd:YAG laser at a centre signal-wave wavelength of 685 nm, one can use a BBO crystal instead of KTP [38 – 40]. In this case, the centre idler-wave wavelength amounts to 2380 nm, a value beyond the absorption range of BBO (which starts above 2550 nm) [35]. BBO crystals are most often used in NOPA to amplify chirped and time-extended femtosecond pulses [41] because they are characterised by very high breakdown threshold (note that one must use crystals about 1 mm thick and, therefore, perform strong focusing of pump radiation into the crystal in order to form a gain band 2000 cm^{-1} wide or even wider). The gain bandwidth of 400 – 500 cm^{-1}, which is required in our case, is obtained in the noncollinear geometry with a KTP crystal 10 mm long; there is no need for strong focusing. Under these conditions, according to [35], the effective nonlinearity of a KTP crystal exceeds that of BBO.

4. Conclusions

We implemented parametric amplification of broadband picosecond radiation of a modeless dye laser in a KTP crystal. The parametric amplifier was pumped by 63-ps second-har-

monic pulses of a Nd:YAG laser. Broadband amplification was obtained due to the group matching upon noncollinear interaction of light waves. Pulses with a duration of 26 ps, an average wavelength of 685 nm, a bandwidth of 21 nm (450 cm^{-1}) and an energy of 1.2 mJ were obtained at 15% conversion of pump energy into the signal-wave energy. These sources of picosecond pulses can be used in different schemes of nonlinear spectroscopy.

References

1. Ball S.M., Langridge J.M., Jones R.L. *Chem. Phys. Lett.*, **398**, 68 (2004).
2. Wu T., Zhao W., Chen W., Zhang W., Gao X. *Appl. Phys. B*, **94**, 85 (2009).
3. Xu F., Liu Z., Zhang Y.G., Somesfalean G., Zhang Z.G. *Appl. Phys. Lett.*, **88**, 231109 (2006).
4. Fiedler S.E., Hese A., Ruth A.A. *Chem. Phys. Lett.*, **371**, 274 (2003).
5. Fiedler S.E., Hoheisel G., Ruth A.A., Hese A. *Chem. Phys. Lett.*, **382**, 447 (2003).
6. Alfano R.R. *Supercontinuum Laser Source* (New York: Springer-Verlag, 1989).
7. Zheltikov A.M. *Optika mikrostrukturirovannykh volokon* (Optics of Microstructured Fibres) (Moscow: Nauka, 2004).
8. Brown D.M., Shi K., Liu Z., Philbrick C.R. *Opt. Express*, **16**, 8457 (2008).
9. Langridge J.M., Laurila T., Watt R.S., Jones R.L., Kaminski C.F., Hult J. *Opt. Express*, **16**, 10178 (2008).
10. Niermann B., Budunglu I.L., Gurel K., Boke M., Ilday F.O., Winter J. *J. Phys. D: Appl. Phys.*, **45**, 245202 (2012).
11. Pomraenke R., Ropers C., Renard J., Lienau C., Luer L., Polli D., Cerullo G. *J. Microscopy*, **229**, 197 (2008).
12. Vidal F., Tadjeddine A. *Rep. Prog. Phys.*, **68**, 1095 (2005).
13. Richter L.J., Petrally-Mallow T.P., Stephenson J.C. *Opt. Lett.*, **23** (20), 1594 (1998).
14. Lagutchev A., Lozano A., Mukherjee H., Hambir S.A., Dlott D. *Acta A Mol. Biomol. Spectrosc.*, **75**, 1289 (2010).
15. Isaenko O., Bourguet E., Vöhringer P. *Opt. Lett.*, **35**, 3832 (2010).
16. Isaenko O., Bourguet E. *Opt. Express*, **20**, 547 (2011).
17. Akhmanov S.A., Koroteev N.I. *Metody nelineinoi optiki v spektroskopii rasseyaniya sveta* (Methods of Nonlinear Optics in Light Scattering Spectroscopy) (Moscow: Nauka, 1981).
18. Eckbreth A.C., Anderson T.J. *Appl. Opt.*, **24**, 2731 (1985).
19. Klauss W., Fabelinsky V.I., Kozlov D.N., Smirnov V.V., Stelmakh O.M., Vereshagin K.A. *Appl. Phys. B*, **70**, 127 (2000).
20. Kozlov D.N., Weikl M.C., Kiefer J., Seeger T., Leipertz A. *Opt. Express*, **16**, 18379 (2008).
21. Ewart P. *Opt. Commun.*, **55** (2), 124 (1985).
22. Roy S., Meyer T.R., Gord J.R. *Appl. Phys. Lett.*, **87**, 264103 (2005).
23. Seeger T., Kiefer J., Leipertz A., Patterson B., Kliewer C.J., Settersten N.B. *Opt. Lett.*, **34** (23), 3755 (2009).
24. Bohlin A., Nordström E., Patterson B.D., Bengtsson P.-E., Kliewer C.J. *J. Chem. Phys.*, **137**, 074302 (2012).
25. Montello A., Nishihara M., Rich J.W., Adamovich I.V., Lempert W.R. *Exp. Fluids*, **54**, 1422 (2013).
26. Richardson D.R., Lucht R.P., Roy S., Kulatilaka W.D., Gord J.R. *Proc. Combust. Inst.*, **33**, 839 (2011).
27. Seeger T., Kiefer J., Gao Y., Patterson B.D., Kliewer C.J., Settersten N.B. *Opt. Lett.*, **35** (12), 2040 (2010).
28. Kliewer C.J., Gao Y., Seeger T., Kiefer J., Patterson B.D., Settersten N.B. *Proc. Combust. Inst.*, **33**, 831 (2011).
29. Kraemer D., Cowan M.L., Hua R., Franjic K., Miller R.J.D. *J. Opt. Soc. Am. B*, **24** (4), 813 (2007).
30. Lozhkarev V.V., Freidman G.I., Ginzburg V.N., Katin E.V., Khazanov E.A., Kirsanov A.V., Luchinin G.A., Mal'shakov A.N.,

Martyanov M.A., Palashov O.V., Poteomkin A.K., Sergeev A.M., Shaykin A.A., Yakovlev I.V. *Las. Phys. Lett.*, **4** (6), 421 (2007).

31. Magnitskii S.A., Malachova V.I., Tarasevich A.P., Tunkin V.G., Yakubovich S.D. *Opt. Lett.*, **11**, 18 (1986).

32. Hsu P.S., Roy S., Gord J.R. *Opt. Commun.*, **281**, 6068 (2008).

33. Gerullo G., Nisoli M., Stagira S., De Silvestri S. *Opt. Lett.*, **23**, 1283 (1998).

34. Shorakawa A., Kobayashi T. *Appl. Phys. Lett.*, **72**, 147 (1998).

35. Nikogosyan D.N. *Appl. Phys. A*, **52**, 359 (1991).

36. Shidlovski V., in *Optical Coherence Tomography*. Ed. by W. Drexler, J.G. Fujimoto (Berlin: Springer-Verlag, 2008) pp 281–300.

37. Andreeva E.V., Il'chenko S.N., Kostin Yu.O., Ladugin M.A., Lapin P.I., Marmalyuk A.A., Yakubovich S.D. *Kvantovaya Elektron.*, **43** (8), 751 (2013) [*Quantum Electron.*, **43** (8), 751 (2013)].

38. Homann C., Breuer M., Setzpfandt F., Pertch T., Riedle E. *Opt. Express*, **21** (1), 730 (2013).

39. Krylov V., Ollikainen O., Gallus J., Wild U., Rebane A., Kalintsev A. *Opt. Lett.*, **23** (2), 100 (1998).

40. Nikolov I., Gaydardzhiev A., Buchvarov I., Tzankov P., Noack F., Petrov V. *Opt. Lett.*, **32** (22), 3342 (2007).

41. Dubietis A., Jonsauskas G., Piskarskas A. *Opt. Commun.*, **88**, 437 (1992).